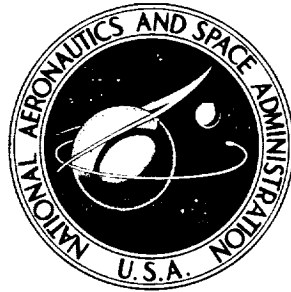


NASA TECHNICAL NOTE



NASA TN D-8029

NASA TN D-8029

CASE FILE COPY

ANALYSIS OF DYNAMIC CAPACITY OF LOW-CONTACT-RATIO SPUR GEARS USING LUNDBERG-PALMGREN THEORY

*John J. Coy, Dennis P. Townsend,
and Erwin V. Zaretsky*

*Lewis Research Center
and U.S. Army Air Mobility R&D Laboratory
Cleveland, Ohio 44135*



NATIONAL AERONAUTICS AND SPACE ADMINISTRATION • WASHINGTON, D. C. • AUGUST 1975



1. Report No. NASA TN D-8029	2. Government Accession No.	3. Recipient's Catalog No.	
4. Title and Subtitle ANALYSIS OF DYNAMIC CAPACITY OF LOW-CONTACT-RATIO SPUR GEARS USING LUNDBERG-PALMGREN THEORY		5. Report Date August 1975	
		6. Performing Organization Code	
7. Author(s) John J. Coy, Dennis P. Townsend, and Erwin V. Zaretsky		8. Performing Organization Report No. E-8164	
		10. Work Unit No. 505-04	
9. Performing Organization Name and Address NASA Lewis Research Center and U. S. Army Air Mobility R&D Laboratory Cleveland, Ohio 44135		11. Contract or Grant No.	
		13. Type of Report and Period Covered Technical Note	
12. Sponsoring Agency Name and Address National Aeronautics and Space Administration Washington, D. C. 20546		14. Sponsoring Agency Code	
		15. Supplementary Notes	
16. Abstract <p>A concise mathematical model is developed for surface fatigue life of low-contact-ratio spur gears. The expected fatigue life of the pinion, gear, or gear sets may be calculated from the model. An equation for the dynamic capacity of the gear set was also derived in terms of the transmitted tangential tooth load which will give a 10-percent fatigue life of one million pinion revolutions. The theoretical life was compared with experimental data for a set of VAR AISI 9310 gears operating at a Hertz stress of 1.71×10^9 newtons per square meter (248 000 psi) and 10 000 revolutions per minute. Good agreement was obtained between the experimental and theoretical surface fatigue life of the gears.</p>			
17. Key Words (Suggested by Author(s)) Spur gears Pitting fatigue life Dynamic capacity		18. Distribution Statement Unclassified - unlimited STAR Category 37 (rev.)	
19. Security Classif. (of this report) Unclassified	20. Security Classif. (of this page) Unclassified	21. No. of Pages 51	22. Price* \$4.25

* For sale by the National Technical Information Service, Springfield, Virginia 22161

1. The first part of the document discusses the importance of maintaining accurate records of all transactions and activities. It emphasizes that this is essential for ensuring transparency and accountability in the organization's operations.

2. The second part of the document outlines the various methods and tools used to collect and analyze data. It highlights the need for consistent data collection procedures and the use of advanced analytical techniques to derive meaningful insights from the data.

3. The third part of the document focuses on the role of technology in data management and analysis. It discusses how modern software solutions can streamline data collection, storage, and analysis processes, thereby improving efficiency and accuracy.

4. The fourth part of the document addresses the challenges associated with data management, such as data quality, security, and privacy. It provides strategies to mitigate these risks and ensure that the data remains reliable and secure throughout its lifecycle.

5. The fifth part of the document concludes by summarizing the key findings and recommendations. It stresses the importance of ongoing monitoring and evaluation to ensure that the data management processes remain effective and aligned with the organization's goals.



CONTENTS

	Page
SUMMARY	1
INTRODUCTION	2
LUNDBERG-PALMGREN THEORY	3
FATIGUE LIFE OF SINGLE PINION TOOTH	4
FATIGUE LIFE OF SINGLE GEAR TOOTH	7
LIFE FOR PINION ALONE	8
LIFE FOR GEAR ALONE	9
LIFE OF GEAR SET IN MESH	10
DYNAMIC CAPACITY OF PINION TOOTH	10
DYNAMIC CAPACITY OF GEAR TOOTH	11
DYNAMIC CAPACITY OF MESH	12
MATERIAL CONSTANTS AND EXPONENTS	13
APPARATUS, SPECIMENS, AND PROCEDURE	14
Gear Test Apparatus	14
Test Lubricant	15
Test Gears	15
Test Procedure	16
RESULTS AND DISCUSSION	16
SUMMARY OF RESULTS	17
APPENDIXES	
A - SYMBOLS	20
B - GEAR GEOMETRY	23
C - STRESS EQUATIONS FOR GEARS IN LINE CONTACT	29
D - MATERIAL CONSTANT	32
E - CALCULATION OF BASIC DYNAMIC CAPACITY AND LIFE OF TEST GEARS	35
REFERENCES	38

[Faint, illegible text covering the majority of the page, likely bleed-through from the reverse side.]



ANALYSIS OF DYNAMIC CAPACITY OF LOW-CONTACT-RATIO SPUR GEARS USING LUNDBERG-PALMGREN THEORY

by John J. Coy, Dennis P. Townsend, and Erwin V. Zaretsky

Lewis Research Center and
U. S. Army Air Mobility R&D Laboratory

SUMMARY

A concise mathematical model for surface fatigue life of low-contact-ratio spur gears was developed. From the model the expected life of the pinion, gear, or gear set may be calculated in terms of pinion revolutions. In addition, an equation for the dynamic capacity of the gear set was derived. The dynamic capacity is defined as the transmitted tangential load carried by the gear set which will cause the 10-percent fatigue life to be one million pinion revolutions.

Experimental gear life data are described for spur gears operating at a Hertz stress of 1.71×10^9 newtons per square meter (248 000 psi) and 10 000 revolutions per minute. The material was vacuum arc remelted (VAR) AISI 9310 heat treated to a Rockwell C hardness of 62.

The theoretical life was compared to the experimentally determined life. Good agreement was obtained when using material constants obtained from life tests of rolling element bearings. A previously determined Weibull slope for gears was used to predict the survival distribution of the current set of gear specimens.

The dynamic capacity of the spur gear mesh W_{tM} is given by

$$W_{tM} = B_1 \cos \varphi \left\{ N_1 \left[1 + \left(\frac{N_1}{N_2} \right)^p \right] \left(\frac{l_1}{\pi} \right)^{\Sigma \rho} f^{(c+h-1)/2} \right\}^{-1/w}$$

and the life L corresponding to a particular transmitted load W_t is given by

$$L = \left(\frac{W_{tM}}{W_t} \right)^p$$

where B_1 is the material constant, φ the pressure angle, N_1 the number of teeth on pinion, N_2 the number of teeth on gear, e the Weibull exponent, l_1 the involute profile arc-length on pinion for the zone of single-tooth contact, $\Sigma \rho$ the curvature sum for the point of highest contact stress, f the face width in contact, and p , c , h , and w are the material constants.

INTRODUCTION

Gears used in aircraft and other applications may fail from scoring, tooth fracture due to bending fatigue, or surface pitting fatigue. The scoring type failure is usually lubrication related and can be corrected by proper lubricant selection and/or changes in gear operating conditions (ref. 1). Tooth breakage is caused by tooth loads which produce bending stresses above the endurance limit of the material (ref. 2). It is usually accepted that the endurance limit, if it does exist, can be predicted from available stress-life (S-N) curves for the material being used (ref. 3). Current methods (ref. 4) of predicting gear surface pitting failures are similar to those used for predicting the bending fatigue limit. According to the method of reference 4, the maximum surface contact stress (Hertz stress) should be limited to a value less than the surface endurance limit of the gear material. It is commonly believed that the gears would then have an infinite surface pitting life. But based on gearing (refs. 5 and 6) and rolling-element bearing life studies (ref. 7), there is no real evidence to support the concept of a surface fatigue limit under normal operating conditions of bearings and gears. Rather, it appears that all gears even if designed properly to avoid failure by scoring and tooth bending fatigue will eventually succumb to surface pitting in much the same way as rolling-element bearings. Even so, as Seireg (ref. 8) points out, the maximum Hertzian stress is a significant parameter that should be kept within bounds if the gear mesh is to have a long enough life. Huffaker (ref. 5) reported that gear life as determined from dynamometer testing of automotive transmissions is dependent on contact stress according to the proportionality

$$\text{Life} \sim \left(\frac{1}{\text{Hertz stress}} \right)^x$$

The failure criterion used was "excessive noise" generated due to pitted gear teeth. For stress levels ranging from 1.4×10^9 to 2.6×10^9 newtons per square meter (200 000 to 380 000 lb/in.²) the stress-life exponent was found to be 6.75. The failure distribution with stress level was reported to be very similar to that of roller bearings with no evidence of an endurance limit (i. e., a stress level for which the gears would have an infinite life). Results of gear testing by Shilke (ref. 6) show similar results for stress levels from 1.4×10^9 to 1.9×10^9 newtons per square meter (210 000 to 280 000 lb/in.²) surface contact stress. Two failure criteria were used: loss of drive and first visible pitting under a $\times 10$ magnification. Both methods gave similar results. In addition to finding that "the pitting fatigue mode of failure appears to have no endurance limit," Shilke concluded that the stress-life exponent is a function of reliability level.

Reference 9 presents a method of determining the allowable stress in gear teeth for infinite life that is consistent with a given level of reliability. However, the method

depends on the concept of a surface fatigue endurance limit and is not consistent with the findings in references 5 and 6.

A recent departure in predicting gear surface (pitting) fatigue life from those of other investigators was that of Rumbarger (ref. 10). Recognizing the similarity in failure between rolling-element bearings and gears, Rumbarger developed a failure model (ref. 10) based on the Lundberg-Palmgren life model (ref. 11) for rolling-element bearings. The Rumbarger model (ref. 10), while a good approach, may have some serious limitations as a design tool. In order to apply the model to life predictions several numerical evaluations of integrals must be carried out. In addition, there is some question regarding the accuracy of the equation as it pertains to the gear tooth profile incorporated in the model, and no full scale gear tests were run to verify the accuracy of the model.

In view of the aforementioned, it becomes the objective of the research reported herein (1) to provide a simplified theory for gear surface (pitting) fatigue failure from which calculations may readily be made to provide life estimates of low contact ratio spur gears and (2) to compare the analytical life prediction with experimental gear life data. The method of analysis is based on the rolling-element fatigue theory contained in reference 11. Simplifications are incorporated into the failure theory for gears based on the observations reported in reference 12, which states that fatigue spalls on gears occurred in the region of highest Hertz stress. Generally, no fatigue failures were observed outside the region of single tooth contact. The results of the theory were compared to experimental gear fatigue results obtained with gears manufactured from AISI 9310 material run at 10 000 rpm, a maximum Hertz stress of 1.71×10^9 newtons per square meter (248 000 psi), and a temperature of 350 K (170^o F).

LUNDBERG-PALMGREN THEORY

The fatigue-life model proposed in 1947 by Lundberg (ref. 11) is the commonly accepted theory to determine the fatigue life of rolling-element bearings. The probability of survival as a function of time or stress cycles is expressed as

$$\log \frac{1}{S} \sim \frac{\tau_0^c \eta^e V}{z_0^h} \quad (1)$$

where

S probability of survival

V volume representation of stress concentration

η millions of stress cycles
 e Weibull exponent
 h, c material dependent exponents
 z_0 depth to critical stress
 τ_0 critical stress

(All symbols are defined in appendix A.) Hence, if the probability of survival is specified, the life η for the required reliability can be considered a function of the stressed volume V , the maximum critical stress τ_0 , and the depth to the critical shearing stress z_0 . As a result, the proportionality can be written as

$$\eta \sim \frac{z_0^{h/e}}{\tau_0^{c/e} V^{1/e}} \quad (2)$$

In applying this relation to gears in contact, the subscript 1 denotes the pinion and 2 denotes the gear. The necessary relations pertaining to gear geometry are given in appendix B, so that the continuity of the derivation is not interrupted.

FATIGUE LIFE OF SINGLE PINION TOOTH

As an expression for the stressed volume in a low contact ratio pinion ($1 < M < 2$), we chose

$$V \sim az_0 l_1 \quad (3)$$

where l_1 is the involute length of the pinion across the heavy load zone. The choice of this length is a simplification of Rumbarger's (ref. 10) use of the entire involute length that passes through the pressure zone. This is a justifiable simplification since operation under lighter loads greatly diminishes the probability of failure. Another reason for choosing the heavily loaded zone is that all observed failures on the NASA gear tests occurred in that zone (mostly where the Hertz load on the pinion is greatest) (ref. 12). It is also assumed that the most severe Hertz stress generated in the contact of the teeth is acting over the entire load zone of single tooth contact.

Equation (1) then becomes

$$\log \frac{1}{S} \sim \frac{\tau_o^c \eta^e a l_1}{z_o^{h-1}} \quad (4)$$

Using equations (C7), (C9), and (C10) from Hertz theory (see appendix C) gives

$$\log \frac{1}{S} \sim \left(\frac{T3Q}{2\pi ab} \right)^c \frac{\eta^e a l_1}{(\xi b)^{h-1}} \quad (5)$$

Since each tooth is stressed only once per revolution, η may represent millions of revolutions of the pinion L . According to appendix B the pinion involute arc length in the heavy load zone is given by

$$l_1 = \Delta l_1 = \frac{r_{b1}}{2} (\theta_{U1}^2 - \theta_{L1}^2) \quad (6)$$

In order that the constants of proportionality and exponents that were found by Lundberg and Palmgren (ref. 11) may be used, the following derivations will be closely compared to their work.

Rearranging equation (5) and dropping the constant $(3/2\pi)^c$ give

$$\log \frac{1}{S} \sim \frac{T^c Q^c L^e l_1}{\xi^{h-1}} \left(\frac{1}{a} \right)^{c-1} \left(\frac{1}{b} \right)^{c+h-1} \quad (7)$$

In order to use the same proportionality constant later introduced by Lundberg and called the "material constant," the l_1 should be divided by π ; the relation is now written as

$$\log \frac{1}{S} \sim \frac{T^c Q^c L^e}{\xi^{h-1}} \left(\frac{l_1}{\pi} \right) \left(\frac{1}{a} \right)^{c-1} \left(\frac{1}{b} \right)^{c+h-1} \quad (8)$$

This equation is valid for both line and point contact. Using the special relations of appendix C ((C5), (C7), and (C12)) for line contact gives the

$$\log \frac{1}{S} \sim \frac{T_o^c}{\xi_o^{h-1}} \left(\frac{\pi E_o \Sigma \rho}{6} \right)^{(c+h-1)/2} \left(\frac{4}{3f} \right)^{(c-1-h)/2} Q^{(c-h+1)/2} \frac{l_1}{\pi} L^e \quad (9)$$

This equation agrees in form with equation (46) of reference 11 if note is taken that

$$D_a^{(c+h-1)/2} D_a^{(c-h-1)/2} \left(\frac{1}{D_a^2} \right)^{(c-h+1)/2} D_a^{2-h} \equiv 1 \quad (10)$$

After assuming the probability of survival $S = S_1 = 0.9$ and designating $L = L_1$ as the corresponding life for a 90-percent survival probability, the equation becomes

$$Q^{(c-h+1)/2} L_1^e \sim \left[\frac{l_1}{\pi} \left(\frac{4}{3f} \right)^{(c-1-h)/2} \left(\frac{\pi E_o \Sigma \rho}{6} \right)^{(c+h-1)/2} \frac{T_o^c}{\xi_o^{h-1}} \right]^{-1} \quad (11)$$

or, since T_o and ξ_o are constant for line contact,

$$Q^{(c-h+1)/2} L_1^e \sim \left[\frac{l_1}{\pi} \Sigma \rho^{(c+h-1)/2} \right]^{-1} f^{(c-1-h)/2} \quad (12)$$

Next, after defining a material constant B_1 and rearranging exponents the form is

$$QL_1^{2e/(c-h+1)} = B_1 \left[\frac{l_1}{\pi} \Sigma \rho^{(c+h-1)/2} \right]^{-2/(c-h+1)} f^{(c-h-1)/(c-h+1)} \quad (13)$$

This equation is consistent with equation (48) of reference 11 where the appropriate definitions are made for f and D_n ; also, because of equation (10) the D_a is dropped.

Finally,

$$QL_1^{(1/p)} = B_1 \left(\frac{l_1}{\pi} \right)^{-2/(c-h+1)} \Sigma \rho^{-(c+h-1)/(c-h+1)} f^{(c-h-1)/(c-h+1)} \quad (14)$$

where

$$p = \frac{c - h + 1}{2e} \quad (15)$$

The life of a single pinion tooth with a 90-percent probability of survival may be determined by using equation (13) and rearranging terms as follows:

$$L_1 = B_1^p \left(\frac{l_1}{\pi} \right)^{-1/e} \Sigma \rho^{-(c+h-1)/2e} f^{(c-h-1)/2e} Q^{-p} \quad (16)$$

Specific values of the material constant and exponents are not substituted into the derivation here in order to maintain generality in the results.

FATIGUE LIFE OF SINGLE GEAR TOOTH

If the appropriate variables are substituted into the life equation for the pinion tooth (eq. (16)), an equation valid for the gear tooth is obtained:

$$L_2 = B_1^p \left(\frac{l_2}{\pi} \right)^{-1/e} \Sigma \rho^{-(c+h-1)/2e} f^{(c-h-1)/2e} Q^{-p} \quad (17)$$

where the life of the gear tooth is written in terms of gear revolutions, and l_2 is the involute length of the gear during the single tooth load region.

The life of the gear tooth in terms of pinion rotations L_{2P} may be related to gear tooth life L_2 by

$$L_{2P} = \frac{N_2}{N_1} L_2 \quad (18)$$

Also for the gear tooth as was done for the pinion tooth in equation (6)

$$l_2 = \frac{r_{b2}}{2} \left(\theta_{U2}^2 - \theta_{L2}^2 \right) \quad (19)$$

By geometry it can easily be shown that

$$\frac{\theta_2}{\theta_1} = \frac{r_1}{r_2} = \frac{N_1}{N_2} = \frac{r_{b1}}{r_{b2}} \quad (20)$$

Therefore,

$$l_2 = \frac{r_{b1}}{2} \frac{N_2}{N_1} \left[\left(\theta_{U1} \frac{N_1}{N_2} \right)^2 - \left(\theta_{L1} \frac{N_1}{N_2} \right)^2 \right] \quad (21)$$

$$l_2 = \frac{N_1}{N_2} l_1 \quad (22)$$

From equations (16), (17), (18), and (22) the life equation for a single gear tooth in terms of pinion rotations is

$$L_{2P} = \left(\frac{N_2}{N_1} \right)^{(1+e)/e} L_1 \quad (23)$$

where it is assumed that the same load Q is acting on both members.

LIFE FOR PINION ALONE

According to the relation for survival probability of a single pinion tooth under constant service conditions

$$\log \frac{1}{S} \sim L^e \quad (24)$$

For a 90-percent survival rate $S = S_1 = 0.90$ and $L = L_1$. If the constant of proportionality K is used, then

$$\log \frac{1}{0.9} = KL_1^e \quad (25)$$

Therefore, for any general survival rate we write

$$\log \frac{1}{S} = \left(\frac{L}{L_1} \right)^e \log \frac{1}{0.9} \quad (26)$$

From basic probability theory, the probability of survival for N_1 teeth is the product of survival probabilities for the individual teeth. Then the probability of survival for the pinion is

$$S_P = S^{N_1} \quad (27)$$

and

$$\log \frac{1}{S_P} = \log \left(\frac{1}{S} \right)^{N_1} = N_1 \log \frac{1}{S} = N_1 \left(\frac{L}{L_1} \right)^e \log \frac{1}{0.9} \quad (28)$$

For a 90-percent survival for the pinion, $S_P = 0.9$, $L = L_P$, and

$$\log \frac{1}{0.9} = N_1 \left(\frac{L_P}{L_1} \right)^e \log \frac{1}{0.9} \quad (29)$$

Then the life for the pinion with a 90-percent survival probability is related to the life of a single tooth by

$$\left(\frac{1}{L_P} \right)^e = N_1 \left(\frac{1}{L_1} \right)^e \quad (30)$$

LIFE FOR GEAR ALONE

Again from the product law, the survival probability for the gear is

$$S_G = S^{N_2} \quad (31)$$

where the relation for a single tooth is

$$\log \frac{1}{S} = \left(\frac{L}{L_2} \right)^e \log \frac{1}{0.9} \quad (32)$$

Then for the gear

$$\log \frac{1}{S_G} = N_2 \log \left(\frac{1}{S} \right) = N_2 \left(\frac{L}{L_2} \right)^e \log \frac{1}{0.9} \quad (33)$$

For a 90-percent survival of the gear $S_G = 0.9$ and $L = L_G$ where L_G is the number of gear rotations endured:

$$\left(\frac{1}{L_G}\right)^e = N_2 \left(\frac{1}{L_2}\right)^e \quad (34)$$

Note that if the life of the gear and gear tooth is given in terms of pinion rotations, then

$$\left(\frac{1}{L_{GP}}\right)^e = N_2 \left(\frac{1}{L_{2P}}\right)^e \quad (35)$$

where L_{GP} is the gear life in terms of pinion rotations and L_{2P} is the life of one gear tooth in terms of pinion rotations.

LIFE OF GEAR SET IN MESH

From probability theory the probability of survival of the two gears in mesh is given by

$$S_M = S_P \cdot S_G \quad (36)$$

and therefore

$$\left(\frac{1}{L_M}\right)^e = \left(\frac{1}{L_P}\right)^e + \left(\frac{1}{L_{GP}}\right)^e \quad (37)$$

For a 90-percent probability of survival for the mesh after L_M million revolutions of the pinion, substituting equations (30) and (35) into equation (37) gives

$$\left(\frac{1}{L_M}\right)^e = N_1 \left(\frac{1}{L_{1P}}\right)^e + N_2 \left(\frac{1}{L_{2P}}\right)^e \quad (38)$$

In this equation it should be noticed that all lives are expressed in the same time base, that is, in terms of pinion rotations.

DYNAMIC CAPACITY OF PINION TOOTH

The dynamic capacity of a single tooth in the pinion is defined as the transmitted tangential load W_{tP} that may be carried for one million pinion revolutions with a

90-percent probability of survival. From equation (14),

$$Q_{c1} = B_1 \left(\frac{l_1}{\pi} \right)^{-2/(c-h+1)} \Sigma \rho^{-(c+h-1)/(c-h+1)} f^{(c-h-1)/(c-h+1)} \quad (39)$$

$$W_{tP} = Q_{c1} \cos \varphi \quad (40)$$

where W_{tP} is the dynamic capacity of a single pinion tooth.

DYNAMIC CAPACITY OF GEAR TOOTH

The dynamic capacity of a single gear tooth is defined as the transmitted tangential load W_{tG} that may be carried for one million pinion revolutions with a 90-percent probability of survival for that gear tooth. From equations (14) and (23) the gear tooth life is

$$L_{2P} = \left(\frac{N_2}{N_1} \right)^{(1+e)/e} \left[B_1 \left(\frac{l_1}{\pi} \right)^{-2/(c-h+1)} \Sigma \rho^{-(c+h-1)/(c-h+1)} f^{(c-h-1)/(c-h+1)} Q^{-1} \right]^p \quad (41)$$

Setting $L_{2P} = 1$ and solving equation (41) for the dynamic capacity give

$$Q_{c2} = \left(\frac{N_2}{N_1} \right)^{(1+e)/ep} B_1 \left(\frac{l_1}{\pi} \right)^{-2/(c-h+1)} \Sigma \rho^{-(c+h-1)/(c-h+1)} f^{(c-h-1)/(c-h+1)} \quad (42)$$

and

$$W_{tG} = Q_{c2} \cos \varphi \quad (43)$$

If equations (15), (39), and (40) are used, the dynamic capacity of a single gear tooth may be related to the dynamic capacity of a pinion tooth by

$$W_{tG} = \left(\frac{N_2}{N_1} \right)^{2(1+e)/(c-h+1)} W_{tP} \quad (44)$$

DYNAMIC CAPACITY OF MESH

In the following derivation the dynamic capacity of the mesh W_{tM} is defined as the transmitted tangential load that may be carried for one million pinion revolutions with a 90-percent probability of survival of both pinion and gear. The probability of the mesh surviving is given by

$$S_M = S_P \cdot S_G = S_1^{N_1} S_2^{N_2} \quad (45)$$

From equation (9) for a given set of gears the survival probability of the single pinion tooth is given by

$$\log \frac{1}{S_1} = k_1 Q^w L^e \quad (46)$$

where

$$w \equiv \frac{c - h + 1}{2}$$

For the single gear tooth,

$$\log \frac{1}{S_2} = k_2 Q^w L^e \quad (47)$$

The probability that the mesh will survive is found from equation (45):

$$\log \frac{1}{S_M} = (N_1 k_1 + N_2 k_2) Q^w L^e \quad (48)$$

In equation (46) if $L = 1$ and $S_1 = 0.9$ then $Q = Q_{c1}$. As a result,

$$\log \frac{1}{0.9} = k_1 Q_{c1}^w$$

In equation (47) if $L = 1$ and $S_2 = 0.9$ then $Q = Q_{c2}$. Thus,

$$\log \frac{1}{0.9} = k_2 Q_{c2}^w$$

In equation (48) if $L = 1$ and $S_M = 0.9$ then $Q = Q_{cM}$. Thus,

$$\log \frac{1}{0.9} = (k_1 N_1 = k_2 N_2) Q_{cM}^w$$

From the previous three relations

$$\left(\frac{1}{Q_{cM}}\right)^w = N_1 \left(\frac{1}{Q_{c1}}\right)^w + N_2 \left(\frac{1}{Q_{c2}}\right)^w \quad (49)$$

The dynamic capacity of the mesh is then

$$W_{tM} = Q_{cM} \cos \varphi \quad (50)$$

From equations (15), (39), (42), (46), (49), and (50), the dynamic capacity of the mesh or the transmitted tangential load that may be carried for 10^6 pinion revolutions with a 90-percent reliability is given by

$$W_{tM} = B_1 \cos \varphi \left\{ N_1 \left[1 + \left(\frac{N_1}{N_2}\right)^e \right] \left(\frac{l_1}{\pi}\right)^{\Sigma \rho^{(c+h-1)/2}} f^{-(c-h-1)/2} \right\}^{-1/w} \quad (51)$$

A proportion is set up using equations (48) and (50) whereby the life corresponding to any transmitted tangential load may be calculated. The relation is

$$L = \left(\frac{W_{tM}}{W_t}\right)^p \quad (52)$$

MATERIAL CONSTANTS AND EXPONENTS

From reference 11 the material constant B was determined from test data on Swedish air-melt bearing steel (61.7 to 64.5 Rockwell C hardness). This material is similar to AISI 52100. The material constant B was determined to be 60 when using the gravitational metric system of units (kg and mm) and a 90-percent probability of survival. From appendix D, the material constant B_1 used in this report was determined to be 117 when using the gravitational metric system of units (kg and mm) and a 90-percent probability of survival. The B_1 is 4.08×10^8 when using the International System (SI) of Units and 102 000 when using the U. S. Customary Units in equation (16).

The exponents e , c , h , and p were also determined from test data in reference 11 for roller bearings with line contact as $e = 3/2$, $c = 10\frac{1}{3}$, $h = 2\frac{1}{3}$, and $p = 3$. In a later paper by Lundberg and Palmgren (ref. 13), the material constant for line contact was changed to $B = 56.2$, and the exponents for line contact in roller bearings were reported as $e = 9/8$, $c = 10\frac{1}{3}$, $h = 2\frac{1}{3}$, and $p = 4$.

A useful method for adjusting the material constant to account for increases in life due to upgraded steels and better lubrication techniques is presented in reference 14. Thus, introducing D as a life adjustment factor instead of changing the material constant from that originally used in reference 13 would change equations (16) and (39) as follows:

$$L_1 = DB_1^p \left(\frac{l_1}{\pi} \right)^{-1/e} \Sigma \rho^{-(c+h-1)/2e} f^{(c-h+1)/2e} Q^{-p} \quad (53)$$

$$Q_{c1} = D^{1/p} B_1 \left(\frac{l_1}{\pi} \right)^{-2/(c-h+1)} \Sigma \rho^{-(c+h-1)/(c-h+1)} f^{(c-h-1)/(c-h+1)} \quad (54)$$

APPARATUS, SPECIMENS, AND PROCEDURE

Gear Test Apparatus

The gear fatigue tests were performed in the NASA Lewis Research Center's gear test apparatus (fig. 1). This test rig uses the four-square principle of applying the test gear load so that the input drive need only overcome the frictional losses in the system.

A schematic of the test rig is shown in figure 2. Oil pressure and leakage flow are supplied to the load vanes through a shaft seal. As the oil pressure is increased on the load vanes inside the slave gear, torque is applied to the shaft. This torque is transmitted through the test gears back to the slave gear where an equal but opposite torque is maintained by the oil pressure. This torque on the test gears, which depends on the hydraulic pressure applied to the load vanes, loads the gear teeth to the desired stress level. The two identical test gears can be started under no load; the load can be applied gradually without changing the running track on the gear teeth.

Separate lubrication systems are provided for the test gears and the main gearbox. The two lubricant systems are separated at the gearbox shafts by pressurized labyrinth seals. Nitrogen was the seal gas. The test gear lubricant is filtered through a 5-micron nominal fiberglass filter. The test lubricant can be heated electrically with an immersion heater. The skin temperature of the heater is controlled to prevent overheating the test lubricant.

A vibration transducer mounted on the gearbox is used to automatically shut off the test rig when a gear-surface fatigue occurs. The gearbox is also automatically shut off if there is a loss of oil flow to either the main gear box or the test gears, if the test gear oil overheats, or if there is a loss of seal gas pressurization.

The test rig is belt driven and can be operated at several fixed speeds by changing pulleys. The operating speed for the tests reported herein was 10 000 rpm.

Test Lubricant

All tests were conducted with a single batch of superrefined naphthenic mineral oil lubricant having proprietary additives (antiwear, antioxidant, and antifoam). The physical properties of this lubricant are summarized in table I. Five percent of an extreme pressure additive, designated Anglamol 81 (partial chemical analysis given in table II), was added to the lubricant. The lubricant flow rate was held constant at 800 cubic centimeters per minute, and the lubrication was supplied to the inlet mesh of the gear set by jet lubrication. The lubricant inlet temperature was constant at 319 ± 6 K ($115^{\circ} \pm 10^{\circ}$ F), and the lubricant outlet temperature was nearly constant at 350 ± 3 K ($170^{\circ} \pm 5^{\circ}$ F). This outlet temperature was measured at the outlet of the test-gear cover. A nitrogen cover gas was used throughout the test as a baseline condition which allowed testing at the same conditions at much higher temperatures without oil degradation. This cover gas also reduced the effect of the oil additives on the gear surface boundary lubrication by reducing the chemical reactivity of the additive-metal system by excluding oxygen (ref. 15).

Test Gears

Test gears were manufactured from vacuum arc remelted (VAR) AISI 9310 case carburized steel to an effective case depth of 1 millimeter (0.040 in.). The material chemical composition is given in table III and the heat treatment schedule is given in table IV. The nominal Rockwell C hardnesses of the case and core were 62 and 45, respectively. This material is a commonly used steel in gear manufacture.

Photomicrographs of the microstructure of the AISI 9310 are shown in figure 3. Figure 3(a) shows the high-carbon fine-grained martensitic structure of the hardened case of the gear. Figure 3(b) shows the core region of the gear with its softer low-carbon refined austenitic grain structure.

Dimensions for the test gears are given in table V. All gears have a nominal surface finish on the tooth face of 0.406 micrometer ($16 \mu\text{in.}$) rms and a standard 20° involute tooth profile.

Test Procedure

The test gears were cleaned to remove the preservative and then assembled on the test rig. The test gears were run in an offset condition with a 0.30-centimeter (0.120-in.) tooth-surface overlap to give a load surface on the gear face of 0.28 centimeter (0.110 in.) of the 0.635-centimeter- (0.250-in. -) wide gear, thereby allowing for an edge radius of the gear teeth. By testing both faces of the gears, a total of four fatigue tests could be run for each set of gears. All tests were run at a load of 1157 newtons per centimeter (661 lb/in.) for 1 hour. The load was then increased to 5784 newtons per centimeter (3305 lb/in.) with a 1.71×10^9 newton per square meter (248 000 psi) pitch-line Hertz stress. At the pitch-line load the tooth bending stress was 24.8×10^8 newtons per square meter (35 100 psi) if plain bending is assumed. However, because there is an offset load there is an additional stress imposed on the tooth bending stress. Combining the bending and torsional moments gives a maximum stress of 26.7×10^8 newtons per square meter (38 700 psi). This bending stress does not consider the effects of tip relief which will also increase the bending stress.

The test gears were operated at 10 000 rpm, which gave a pitch-line velocity of 46.55 meters per second (9163 ft/min). A lubricant was supplied to the inlet mesh at 800 cubic centimeters per minute (0.21 gal/min) at 319 ± 6 K (115 ± 10 ° F). The tests were continued 24 hours a day until they were shut down automatically by the vibration-detection transducer located on the gearbox, adjacent to the test gears. The lubricant was circulated through a 5-micron fiberglass filter to remove wear particles. A total of 3800 cubic centimeters (1 gal) of lubricant was used for each test; the lubricant was discarded, along with the filter element, after each test. Inlet and outlet oil temperatures were recorded continuously on a strip-chart recorder.

The pitch-line elastohydrodynamic (EHD) film thickness was calculated by the method of reference 16. It was assumed, for this film thickness calculation, that the gear temperature at the pitch line was equal to the outlet oil temperature and that the inlet oil temperature to the contact zone was equal to the gear temperature, even though the oil inlet temperature was considerably lower. It is probable that the gear surface temperature could be even higher than the oil outlet temperature, especially at the end points of sliding contact. The EHD film thickness for these conditions was computed to be 0.65 micrometer (26 μ in.), which gave a ratio of film thickness to composite surface roughness (h/σ) of 1.13.

RESULTS AND DISCUSSION

Gear fatigue tests were conducted with gears made from vacuum arc remelt (VAR) AISI 9310 steel. Test conditions were a load of 5784 newtons per centimeter (3305

lb/in.), which produced a maximum Hertz stress at the pitch line of 1.71×10^9 newtons per square meter (248 000 psi), a test speed of 10 000 rpm, and a gear temperature of 350 K (170° F). A superrefined naphthenic mineral oil was the lubricant. Failure of the gears occurred due to surface fatigue pitting. Test results were statistically evaluated using the methods of reference 17. The results of these tests are plotted on Weibull coordinates in figure 4. Weibull coordinates are the log-log of the reciprocal of the probability of survival graduated as the statistical percent of specimens failed (ordinate) against the log of time to failure or system life (abscissa). The experimental 10-percent life or the lift at a 90-percent probability of survival was 11.4 million revolutions or 19 hours of operation.

The theoretical 10-percent life for this set of conditions was calculated using equation (42) and the exponents $h = 2\frac{1}{3}$, $c = 10\frac{1}{3}$, $e = 3$, and constant $B_1 = 102\ 000$. The calculated 10-percent life was 32 million revolutions or 53 hours (see appendix E) where h , c , and B_1 are based on rolling element bearing experience and the Weibull slope e is based on gear tests reported in references 5, 6, and 12.

It should be stated here that the Weibull slope e was assumed to be independent of the stress level and reliability level S in the original work referenced (ref. 11). There is some evidence suggested in reference 6 showing that the exponent e is dependent on the stress level. However, the value of e used previously is representative of data by Shilke (ref. 6) and other NASA tests where the stress level was the same as in the tests reported here.

The predicted life can be considered a reasonably good engineering approximation to the experimental life results. However, the theoretical prediction does not consider material and processing factors such as material type, melting practice, or heat treatment - nor does it consider environmental factors such as lubrication and temperature. All these factors are known to be extremely important in their effect on rolling-element bearing life (ref. 14). There is no reason why these effects to determine gear life should be significantly different from those used to determine bearing life. More test data obtained with gear specimens under various test conditions and different materials and lubricants are required to establish and/or affirm the material constant B_1 and the exponents c , h , and e for gears. However, the results presented herein support the use of the statistical methods presented for predicting spur gear fatigue life with a standard involute profile.

SUMMARY OF RESULTS

An analytical model was developed to determine the fatigue life and dynamic capacity of low contact ratio spur gears. The analytical results were compared with experi-

mental gear life data obtained with a group of vacuum arc remelted (VAR) AISI 9310 spur gears. The test gears had a standard 20° involute profile and a 8.89-centimeter (3.5-in.) pitch diameter. Test conditions were a maximum Hertz stress of 1.71×10^9 newtons per square meter (248 000 psi), a speed of 10 000 rpm, and a temperature of 350 K (170° F). The lubricant was a superrefined naphthenic mineral oil with an additive package. The following results were obtained:

1. There was good agreement between the predicted gear mesh life and the experimental life results.
2. The experimentally determined Weibull slope e for a sample of spur gears and the material constant B_1 and exponents h and c from roller bearing life tests were used successfully to predict gear life. However, further experimental work is needed to give statistical significance to those exponents and the material constant.
3. The dynamic capacity of the spur gear mesh is given by

$$W_{tM} = B_1 \cos \varphi \left\{ N_1 \left[1 + \left(\frac{N_1}{N_2} \right)^e \right] \left(\frac{l_1}{\pi} \right)^{\Sigma \rho^{(c+h-1)/2} f^{-(c-h-1)/2}} \right\}^{-1/w}$$

and the life corresponding to a particular transmitted load is given by

$$L = \left(\frac{W_{tM}}{W_t} \right)^p$$

where

B_1	material constant
φ	pressure angle
N_1	number of teeth on pinion
N_2	number of teeth on gear
e	Weibull exponent
l_1	involute profile arc-length on pinion for zone of single-tooth contact
$\Sigma \rho$	curvature sum for point of highest contact stress

f face width in contact

p, c, h, w material constants

Lewis Research Center,
National Aeronautics and Space Administration,
and
U. S. Army Air Mobility R&D Laboratory,
Cleveland, Ohio, March 26, 1975,
505-04.

APPENDIX A

SYMBOLS

a	half of major axis of Hertzian contact, m (in.)
B	material constant defined by eq. (116) of ref. 11
B_1	material constant defined by eq. (13)
b	half of minor axis of Hertzian contact, m (in.)
C	gear center distance, m (in.)
c	orthogonal shear stress exponent
D	life improvement factor defined by eq. (53)
D_a	rolling element diameter, m (in.)
D_n	raceway diameter (in direction of rolling), m (in.)
d_m	pitch diameter of roll bodies
E	Young's modulus, N/m^2 (psi)
E_o	defined by eq. (C3)
e	Weibull exponent
f	face width of tooth, m (in.)
h	depth to critical stress exponent
K, k_1, k_2	proportionality constants
L	life in millions of revolutions
l	involute profile arc length, m (in.)
M	contact ratio
N	number of teeth
P	diametral pitch, teeth/m (teeth/in.)
p	load-life exponent defined by eq. (15)
P_b	base pitch, m/tooth (in./tooth)
P_c	circumferential pitch, m/tooth (in./tooth)
Q	load normal to involute profile, N (lb)
Q_c	dynamic capacity for normal loading, N (lb)
r	pitch circle radius, m (in.)

r_a	addendum circle radius, m (in.)
r_b	base circle radius, m (in.)
S	probability of survival
T	defined in eq. (C11)
U	number of contact cycles per bearing revolution
V	volume, m^3 (in. ³)
W_t	transmitted tangential load, N (lb)
w	defined by eq. (50)
Z	contact path length, m (in.)
z_o	depth of occurrence of critical shearing stress, m (in.)
α	angle of approach, rad
α'	angle of recess, rad
$\bar{\alpha}$	contact angle, rad
β	contact roll angle, rad
γ	total contact roll angle, rad
δ	precontact roll angle, rad
Z	number of roll bodies per row
ζ	defined in eq. (C10)
η	millions of stress cycles
θ_L	base circle roll angle at entry to single tooth load zone, rad
θ_U	base circle roll angle at exit from single tooth load zone, rad
θ_1	pinion base circle roll angle, rad
μ, ν	defined in eq. (C2)
ρ	curvature radius, m (in.)
$\Sigma\rho$	curvature sum, m^{-1} (in. ⁻¹)
τ_o	maximum subsurface orthogonal reversing shear stress, N/m^2 (psi)
φ	pressure angle, rad

Subscripts:

G	gear
H	high load

- L low load
- M mesh of pinion and gear
- P pinion
- 1 reference to driving member, pinion
- 2 reference to driven gear

APPENDIX B

GEAR GEOMETRY

CALCULATION OF PINION INVOLUTE ARC LENGTH AS

FUNCTION OF PINION ROLL ANGLE

The radius of curvature at point A is $r_{b1}\theta_1$, the arc length along the involute is l , and the differential element of arc length dl is $(dx^2 + dy^2)^{1/2}$. The coordinates of a typical point on the involute are (x, y) for the roll angle θ_1 (fig. 5):

$$\begin{aligned} x &= r_{b1} \sin \theta_1 - \overline{t_1 A} \cos \theta_1 \\ &= r_{b1} \sin \theta_1 - r_{b1}\theta_1 \cos \theta_1 \\ &= r_{b1}(\sin \theta_1 - \theta_1 \cos \theta_1) \end{aligned} \tag{B1}$$

$$\begin{aligned} y &= -r_{b1} + r_{b1} \cos \theta_1 + \overline{t_1 A} \sin \theta_1 \\ &= -r_{b1} + r_{b1} \cos \theta_1 + r_{b1}\theta_1 \sin \theta_1 \\ &= r_{b1}(\cos \theta_1 + \theta_1 \sin \theta_1 - 1) \end{aligned} \tag{B2}$$

$$\begin{aligned} dx &= r_{b1}(\cos \theta_1 d\theta_1 - d\theta_1 \cos \theta_1 + \theta_1 \sin \theta_1 d\theta_1) \\ &= r_{b1}\theta_1 \sin \theta_1 d\theta_1 \end{aligned}$$

$$\begin{aligned} dy &= r_{b1}(-\sin \theta_1 d\theta_1 + d\theta_1 \sin \theta_1 + \theta_1 \cos \theta_1 d\theta_1) \\ &= r_{b1}\theta_1 \cos \theta_1 d\theta_1 \end{aligned}$$

$$dl = \sqrt{(r_{b1}\theta_1 \sin \theta_1 d\theta_1)^2 + (r_{b1}\theta_1 \cos \theta_1 d\theta_1)^2} = r_{b1}\theta_1 d\theta_1 \tag{B3}$$

After integrating between any two angular positions of the pinion, the increment of involute length is

$$\Delta l_1 = \frac{r_{b1}}{2} (\theta_{U1}^2 - \theta_{L1}^2) \quad (B4)$$

Calculation of Base Pitch

The base pitch p_b is defined as the distance between teeth along the pressure line. Base pitch is also the distance from a point on one tooth to the corresponding point on the next tooth measured along the base circle (see fig. 6):

$$\text{Base pitch} = p_b = \frac{2\pi r_{b1}}{N_1} = \frac{2\pi r_{b1} \cos \varphi}{N_1} = p_c \cos \varphi \quad (B5)$$

Contact Ratio

The path of contact Z is the distance between where the two addendum circles cross the pressure line as shown in figure 7:

$$\text{Addendum radius} = r + \frac{1}{P}$$

$$Z = \overline{eg}$$

$$\overline{et}_2 = \sqrt{\left(r_2 + \frac{1}{P}\right)^2 - (r_2 \cos \varphi)^2}$$

$$\overline{ft}_2 = r_2 \sin \varphi$$

$$\overline{ef} = \sqrt{\left(r_2 + \frac{1}{P}\right)^2 - (r_2 \cos \varphi)^2} - r_2 \sin \varphi$$

Similarly,

$$\overline{fg} = \sqrt{\left(r_1 + \frac{1}{P}\right)^2 - (r_1 \cos \varphi)^2} - r_1 \sin \varphi$$

Let

$$C = \text{Center distance} = r_1 + r_2$$

$$Z = \sqrt{\left(r_1 + \frac{1}{P}\right)^2 - (r_1 \cos \varphi)^2} + \sqrt{\left(r_2 + \frac{1}{P}\right)^2 - (r_2 \cos \varphi)^2} - C \sin \varphi \quad (\text{B6})$$

The contact ratio M is defined as the average number of gear teeth in contact at one time. It is calculated by

$$M = \frac{Z}{P_b}$$

When two teeth are in contact the load is assumed to be equally shared by the teeth. For low contact ratio gears ($1 < M < 2$) there are three load zones. The first occurs as the teeth are coming into contact. At that instant there is also another pair of teeth in contact on the line of action. When the contact occurs near the pitch point there is only one pair of teeth in contact and the total load is carried by a single pair of teeth. The third zone is similar to the first and occurs when the teeth come out of contact. The zones are shown in figure 8.

Two sets of teeth are in contact during roll angles β_L and only one set during roll angle β_H . In the figures 9 and 10 two teeth on each gear are shown by their contacting face profile only. There are two positions shown: with teeth coming into contact in figure 9 and teeth going out of contact in figure 10.

The roll angle for which two teeth are in contact is calculated by

$$\beta_{L1} = \frac{Z - P_b}{r_{b1}} \quad (\text{B7})$$

And the heavily loaded zone β_{H1} may be computed by subtracting the two lightly loaded zone angles from the total contact angle:

$$\beta_{H1} = \gamma_1 - 2\beta_{L1} = \frac{Z - 2(Z - P_b)}{r_{b1}} = \frac{2P_b - Z}{r_{b1}} \quad (\text{B8})$$

Calculation of Angles of Approach and Recess

The angle of approach α is the angle between a line joining the gear centers and a second line which is drawn from the gear center to the intersection of the involute profile with the pitch circle. This intersection is chosen for the instant when the gears are coming into contact as shown in figure 11. Angles of approach may be defined for each gear; in general, $\alpha_1 \neq \alpha_2$.

As the pinion rotates through angle α_1 point e will advance to point f; that is, the contact point will move along the line of action:

$$\overline{ef} = \overline{et}_2 - \overline{ft}_2 = \sqrt{\left(r_2 + \frac{1}{P}\right)^2 - (r_2 \cos \varphi)^2} - r_2 \sin \varphi$$

Also, since the line of action can be thought of as a string being wound onto the base circles as the gears turn in mesh,

$$\overline{ef} = r_{b1} \alpha_1$$

The previous two equations may be solved to give the approach angles for the pinion and gear:

$$\left. \begin{aligned} \alpha_1 &= \frac{\sqrt{\left(r_2 + \frac{1}{P}\right)^2 - (r_2 \cos \varphi)^2} - r_2 \sin \varphi}{r_{b1}} \\ \alpha_2 &= \frac{r_1 \alpha_1}{r_2} \end{aligned} \right\} \quad (\text{B9})$$

The angle of recess α' is defined as the angle included between the line of centers and the line from the gear center to the intersection of the involute profile with the pitch circle at the instant when the gears are going out of mesh as shown in figure 12.

The rotation angle α'_1 of the pinion will wrap the length \overline{fg} of the line of action onto the base circle so

$$\alpha'_1 = \frac{\overline{fg}}{r_{b1}}$$

But

$$\overline{fg} = \overline{t_1g} - \overline{t_1f} = \sqrt{\left(r_1 + \frac{1}{P}\right)^2 - (r_1 \cos \varphi)^2} - r_1 \sin \varphi$$

Therefore,

$$\alpha'_1 = \frac{\sqrt{\left(r_1 + \frac{1}{P}\right)^2 - (r_1 \cos \varphi)^2} - r_1 \sin \varphi}{r_{b1}} \quad \left. \vphantom{\alpha'_1} \right\} \quad (B10)$$

and

$$\alpha'_2 = \frac{r_1 \alpha'_1}{r_2}$$

The total angle of contact is

$$\gamma_1 = \alpha_1 + \alpha'_1$$

Finally, δ_1 is defined as the angle of roll that will bring the pinion tooth from the base point to a contact with the mating gear tooth (fig. 13):

$$\delta_1 = \frac{\overline{et_1}}{r_{b1}}$$

But

$$\overline{et_1} = \overline{t_1t_2} - \overline{et_2}$$

where

$$\overline{t_1t_2} = r_1 \sin \varphi + r_2 \sin \varphi = C \sin \varphi$$

and

$$\overline{et}_2 = \left[\left(r_2 + \frac{1}{P} \right)^2 - (r_2 \cos \varphi)^2 \right]^{1/2}$$

Therefore,

$$\delta_1 = \frac{C \sin \varphi - \sqrt{\left(r_2 + \frac{1}{P} \right)^2 - (r_2 \cos \varphi)^2}}{r_{b1}} \quad (\text{B11})$$

Also note that

$$\frac{\overline{t}_1 f}{r_{b1}} = \delta_1 + \alpha_1 = \tan \varphi \quad (\text{B12})$$

which is evident from figure 13. The required angles defining the length of the most heavily loaded length of the involute profile may be written by referring to figure 8. The needed equations are

$$\theta_{L1} = \delta_1 + \beta_{L1} \quad (\text{B13})$$

$$\theta_{U1} = \theta_{L1} + \beta_{H1} \quad (\text{B14})$$

APPENDIX C

STRESS EQUATIONS FOR GEARS IN LINE CONTACT

The curvature sum in terms of pinion roll angle (fig. 14) is determined first:

$$\Sigma\rho = \frac{1}{\rho_1} + \frac{1}{\rho_2}$$

where

$$\rho_1 = r_{b1}\theta_1$$

$$\rho_2 = \overline{t_1 t_2} - \rho_1 = C \sin \varphi - r_{b1}\theta_1$$

$$\Sigma\rho = \frac{1}{r_{b1}\theta_1} + \frac{1}{C \sin \varphi - r_{b1}\theta_1} = \frac{C \sin \varphi - r_{b1}\theta_1 + r_{b1}\theta_1}{r_{b1}\theta_1(C \sin \varphi - r_{b1}\theta_1)} = \frac{C \sin \varphi}{r_{b1}\theta_1(C \sin \varphi - r_{b1}\theta_1)} \quad (C1)$$

It was determined in reference 11 that

$$\left. \begin{aligned} a &= \mu \sqrt[3]{\frac{3Q}{E_o \Sigma\rho}} \\ b &= \nu \sqrt[3]{\frac{3Q}{E_o \Sigma\rho}} \end{aligned} \right\} \quad (C2)$$

where a and b are the major and minor half axes of the contact ellipse and

$$E_o = \frac{m^2 E}{m^2 - 1} \quad (C3)$$

where $1/m$ is Poisson's ratio.

Thomas and Hoersch (ref. 18) have shown that when line contact is approached in the limit ($a \rightarrow \infty$, $Q \rightarrow \infty$) the general equations for point contact may be extended for that case. With appropriate changes in notation from their equation (84) it is found that

$$\frac{2\pi b^2 a}{3Q} = \frac{\pi b^2}{2} \frac{f}{Q} \quad (C4)$$

From this it follows that for a uniform distribution of pressure on the face of the gear the semimajor axis may be taken as

$$a = \frac{3}{4} f \quad (C5)$$

Also, from reference 18 it can be shown that

$$\lim_{b/a \rightarrow 0} \mu \nu^2 = \frac{2}{\pi} \quad (C6)$$

By using equations (C2), (C5), and (C6) we calculate b as

$$b = \sqrt{\frac{8Q}{\pi f E_o \Sigma \rho}} \quad (C7)$$

Equations (C5) and (C7) are used in the development of equation (9) in the report.

For the general case of point contact the maximum contact stress occurs at the ellipse center and is given by

$$q = \frac{3Q}{2\pi ab} \quad (C8)$$

where Q is the normal load applied to the body. For the line contact situation in gears the maximum Hertz stress on the surface is

$$q = \frac{2Q}{\pi fb} \quad (C9)$$

According to reference 11 the cause of fatigue flaking of bearings is the maximum reversing orthogonal shear stress that occurs at a depth z_o below the surface and has an amplitude that varies between $\pm\tau_o$ where

$$z_o = \zeta b \quad (C10)$$

$$\tau_o = Tq \quad (C11)$$

In general, ζ and T depend on the shape of the contact ellipse and for the special case of line contact

$$\left. \begin{aligned} \frac{b}{a} &= 0 \\ T_0 &= 0.2500 \\ \zeta_0 &= 0.5000 \end{aligned} \right\} \quad (C12)$$

If nonferrous gear materials are used, then the contact dimensions a and b and the stress field parameters T and ζ will change due to the change in E_0 for the different material.

APPENDIX D

MATERIAL CONSTANT

The tests run by Lundberg and Palmgren for SKF bearing steel (AISI 52100) with Rockwell C hardnesses of 61.7 to 64.5 yield a material constant of

$$B = 60 \text{ (kg-mm units)}$$

for the dynamic capacity of line contact given by equation (116) of reference 11:

$$Q_c = \frac{B \left(1 \mp \frac{D_a \cos \bar{\alpha}}{d_m}\right)^{29/27} \left(\frac{D_a}{d_m}\right)^{2/9} D_a^{29/27} l_a^{7/9} Z^{-1/3}}{\left(1 \pm \frac{D_a \cos \bar{\alpha}}{d_m}\right)^{1/3}} \quad (D1)$$

Equation (D1) is valid for a roller bearing. The task now is to find the value of B_1 to be used in the dynamic capacity equation for gears which will be applicable for U. S. Customary (lb and in.) units. In order to simplify the referencing of equations from the work of Lundberg and Palmgren all numbered equations in this appendix refer to the numerations used in reference 11. According to equation (58) of reference 11,

$$Q_c = B_1 (D_a \Sigma \rho)^{-35/27} \left(\frac{D_a}{D_n}\right)^{2/9} u^{-1/3} D_a^{29/27} l_a^{7/9} \quad (D2)$$

Then with equation (107)

$$u = \frac{Z}{2} \left(1 \pm \frac{D_a}{d_m} \cos \bar{\alpha}\right) \quad (D3)$$

and equation (106) where $F(b/a) = 1$ for line contact ($b/a = 0$) gives

$$D_a \Sigma \rho = \frac{2}{1 \mp \frac{D_a \cos \bar{\alpha}}{d_m}} \quad (D4)$$

Using equations (D3) and (D4) in equation (D2) gives

$$Q_c = B_1 \left(\frac{2}{1 \mp \frac{D_a \cos \bar{\alpha}}{d_m}} \right)^{-35/27} \left(\frac{D_a}{D_n} \right)^{2/9} \left[\frac{Z}{2} \left(1 \pm \frac{D_a \cos \bar{\alpha}}{d_m} \right) \right]^{-1/3} D_a^{29/27} l_a^{7/9} \quad (D5)$$

From equations (103) and (104)

$$D_n = d_m \left(1 \pm \frac{D_a \cos \bar{\alpha}}{d_m} \right) \quad (D6)$$

After substituting equation (D6) into (D5) the result is

$$Q_c = \left(B_1 \frac{2^{1/3}}{2^{35/27}} \right) \frac{\left(1 \mp \frac{D_a \cos \bar{\alpha}}{d_m} \right)^{29/27}}{\left(1 \pm \frac{D_a \cos \bar{\alpha}}{d_m} \right)^{1/3}} \left(\frac{D_a}{d_m} \right)^{2/9} D_a^{29/27} l_a^{7/9} Z^{-1/3} \quad (D7)$$

Therefore,

$$B_1 \frac{2^{1/3}}{2^{35/27}} = 60$$

$$B_1 = 116.95$$

This concludes the determination of B_1 . Equation (D2) may be written as

$$Q_c (\text{kg}) = 116.95 (D_a \Sigma \rho)^{-35/27} \left(\frac{D_a}{D_n} \right)^{2/9} u^{-1/3} [D_a (\text{mm})]^{29/27} [l_a (\text{mm})]^{7/9} (\text{kg}) \quad (D9)$$

If conversion factors are used in equation (D9), the value of B_1 which is valid for U. S. Customary Units (lbf and in.) may be determined:

$$Q_c(\text{lb}) = \frac{1 \text{ lb}}{0.4536 \text{ kg}} \times 116.95 \times (D_a \Sigma \rho)^{-35/27} \frac{D_a^{2/9}}{D_n} u^{-1/3}$$

$$\times \left[D_a(\text{in.}) \times \frac{25.4 \text{ mm}}{\text{in.}} \right]^{29/27} \left[l_a(\text{in.}) \times \frac{25.4 \text{ mm}}{\text{in.}} \right]^{7/9} (\text{kg}) \quad (\text{D10})$$

Therefore,

$$B_1 = \frac{(116.95)(25.4)^{50/27}}{(0.4536)} = 102\,000 \text{ (U. S. Customary (lb-in.) Units)} \quad (\text{D11})$$

Similarly, $B_1 = 4.08 \times 10^8$ when SI units (N-m) are used. In a later publication (ref. 13) Lundberg and Palmgren report a material constant B of 56.2. When this is reduced as the value of 60 was before, then the material constant $B_1 = 95\,500$ (U. S. Customary (lb-in.) Units) or 3.82×10^8 (SI units (N-m)) results.

APPENDIX E

CALCULATION OF BASIC DYNAMIC CAPACITY AND LIFE OF TEST GEARS

Gear data:

$$N_1 = N_2 = 28$$

$$f = 0.00279 \text{ m (0.11 in.)}$$

$$C = 0.08890 \text{ m (3.500 in.)}$$

$$P = 8$$

$$r_1 = r_2 = 0.04445 \text{ m (1.750 in.)}$$

Test load:

$$W_t = 1615 \text{ N (363 lb)}$$

Material constants:

$$B_1 = 102\,000$$

$$c = 10\frac{1}{3}$$

$$h = 2\frac{1}{3}$$

$$e = 3$$

From figure 7,

$$r_{b2} = r_{b1} = r_1 \cos \varphi = 0.04177 \text{ m (1.6444 in.)}$$

By equation (B11),

$$\delta_1 = 0.180186 \text{ rad}$$

By equation (B5),

$$p_b = 0.009373 \text{ m (0.369016 in.)}$$

By equation (B6),

$$Z = 0.015353 \text{ m (0.604450 in.)}$$

By equation (B7),

$$\beta_{L1} = 0.143168 \text{ rad}$$

By equation (B13),

$$\theta_{L1} = 0.323354 \text{ rad}$$

By equation (B8),

$$\beta_{H1} = 0.081232 \text{ rad}$$

By equation (B14),

$$\theta_{U1} = 0.404585 \text{ rad}$$

The worst Hertzian stress is considered to occur at the lowest point of single tooth contact on the pinion. Therefore, the curvature sum is calculated for that point, and the stress is assumed to be constant while only one pair of teeth are in contact. By equation (C1),

$$\Sigma\rho = 133.2 \text{ m}^{-1} (3.383627 \text{ in.}^{-1})$$

By equation (6),

$$l_1 = 0.001235 \text{ m (0.048620 in.)}$$

By equation (46),

$$w = 4.5$$

By equation (51),

$$W_{tM} = 16284 \text{ N (3660.81 lb)}$$

By equation (15),

$$p = 1.5$$

By equation (52),

$$L = 32.03 \text{ million revolutions of the pinion}$$

REFERENCES

1. Borsof, V. N.: On the Mechanism of Gear Lubrication. *J. Basic Engr.*, vol. 81, no. 1, Mar. 1959, pp. 79-93.
2. Seabrook, John B.; and Dudley, Darle W.: Results of Fifteen-Year Program of Flexural Fatigue Testing of Gear Teeth. *J. Engr. Ind.*, vol. 86, no. 3, Aug. 1964, pp. 221-239.
3. Rating the Strength of Spur Gear Teeth. AGMA 220.02, American Gear Manufacturers Assoc., 1966.
4. Surface Durability (Pitting) of Spur Gear Teeth. AGMA 210.02, American Gear Manufacturers Assoc., 1965.
5. Huffaker, G. E.: Compressive Failures in Transmission Gearing. *SAE Trans.*, vol. 68, 1960, pp. 53-59.
6. Shilke, W. E.: The Reliability Evaluation of Transmission Gears. SAE Paper 670725, Sept. 1967.
7. Bisson, Edmond E.; and Anderson, William J.: Advanced Bearing Technology. NASA SP-38, 1964, pp. 383-386.
8. Seireg, A.; and Conry, T.: Optimum Design of Gear Systems for Surface Durability. *ASLE Trans.*, vol. 11, no. 4, Oct. 1968, pp. 321-329.
9. Hayashi, Kunikazu; Aiuchi, Susumu; and Anno, Yoshiro: Allowable Stresses in Gear Teeth Based on the Probability of Failure. ASME Paper 72-PTG-45, Oct. 1972.
10. Rumbarger, J. H.; and Leonard, L.: Derivation of a Fatigue Life Model for Gears. FIRL-F-C2864, Franklin Inst. (AD-744504; USAAMRDL-TR-72-14), 1972.
11. Lundberg, G.; and Palmgren, A.: Dynamic Capacity of Rolling Bearings. *ACTA Polytechnica, Mechanical Engineering Series*, vol. 1, no. 3, 1947.
12. Townsend, Dennis P.; Chevalier, James L.; and Zaretsky, Erwin V.: Pitting Fatigue Characteristics of AISI M-50 and Super Nitralloy Spur Gears. NASA TN D-7261, 1973.
13. Lundberg, G.; and Palmgren, A.: Dynamic Capacity of Roller Bearings. *ACTA Polytechnica, Mechanical Engineering Series*, vol. 2, no. 4, 1952.
14. Bamberger, E. N.; Harris, T. A.; Kacmarsky, W. M.; Moyer, C. A.; Parker, R. J.; Sherlock, J. J.; and Zaretsky, E. V.: Life Adjustment Factors for Ball and Roller Bearings. *An Engineering Design Guide*. American Society of Mechanical Engineers, 1971.

15. Fein, R. S.; and Kreuz, K. L.: Chemistry of Boundary Lubrication of Steel by Hydrocarbons. ASLE Trans., vol. 8, no. 1, Jan. 1965, pp. 29-38.
16. Dowson, D.; and Higginson, G. R.: Elasto-Hydrodynamic Lubrication. Pergamon Press, 1966.
17. Johnson, Leonard G.: The Statistical Treatment of Fatigue Experiments. Elsevier Publishing Company, 1964.
18. Thomas, H. R.; and Hoersch, V. A.: Stresses Due to the Pressure of One Elastic Solid upon Another. Univ. Ill. Eng. Experiment Station Bull., vol. 27, no. 46, July 15, 1930.

TABLE I. - PROPERTIES OF SUPERREFINED, NAPHTHENIC,
MINERAL-OIL TEST LUBRICANT

Kinematic viscosity, cm ² /sec (cS) at	
266 K (20 ^o F)	2812×10 ⁻² (2812)
311 K (100 ^o F)	73×10 ⁻² (73)
372 K (210 ^o F)	7.7×10 ⁻² (7.7)
477 K (400 ^o F)	1.6×10 ⁻² (1.6)
Flash point, K (°F)	489 (420)
Autoignition temperature, K (°F)	664 (735)
Pour point, K (°F)	236 (-35)
Density at 289 K (60 ^o F), g/cm ³	0.8899
Vapor pressure at 311 K (100 ^o F), mm Hg (or torr)	0.01
Thermal conductivity at 311 K (100 ^o F), J/(m)(sec)(K) (Btu/(hr)(ft)(°F))	0.04 (0.0725)
Specific heat at 311 K (100 ^o F), J/(kg)(K) (Btu/(lb)(°F))	582 (0.450)

TABLE II. - PROPERTIES OF LUBRICANT ADDITIVE ANGLAMOL 81

Percent phosphorous by weight	0.66
Percent sulfur by weight	13.41
Specific gravity	0.982
Kinematic viscosity at 372 K (210 ^o F), cm ² /sec (cS)	29.5×10 ⁻² (29.5)

TABLE III. - CHEMICAL COMPOSITION OF VAR AISI 9310

GEAR MATERIALS BY PERCENT WEIGHT

Element	C	Mn	Si	Ni	Cr	Mo	Cu	P and S
Weight percent	0.10	0.63	0.27	3.22	1.21	0.12	0.13	0.005

TABLE IV. - HEAT TREATMENT PROCESS FOR VACUUM

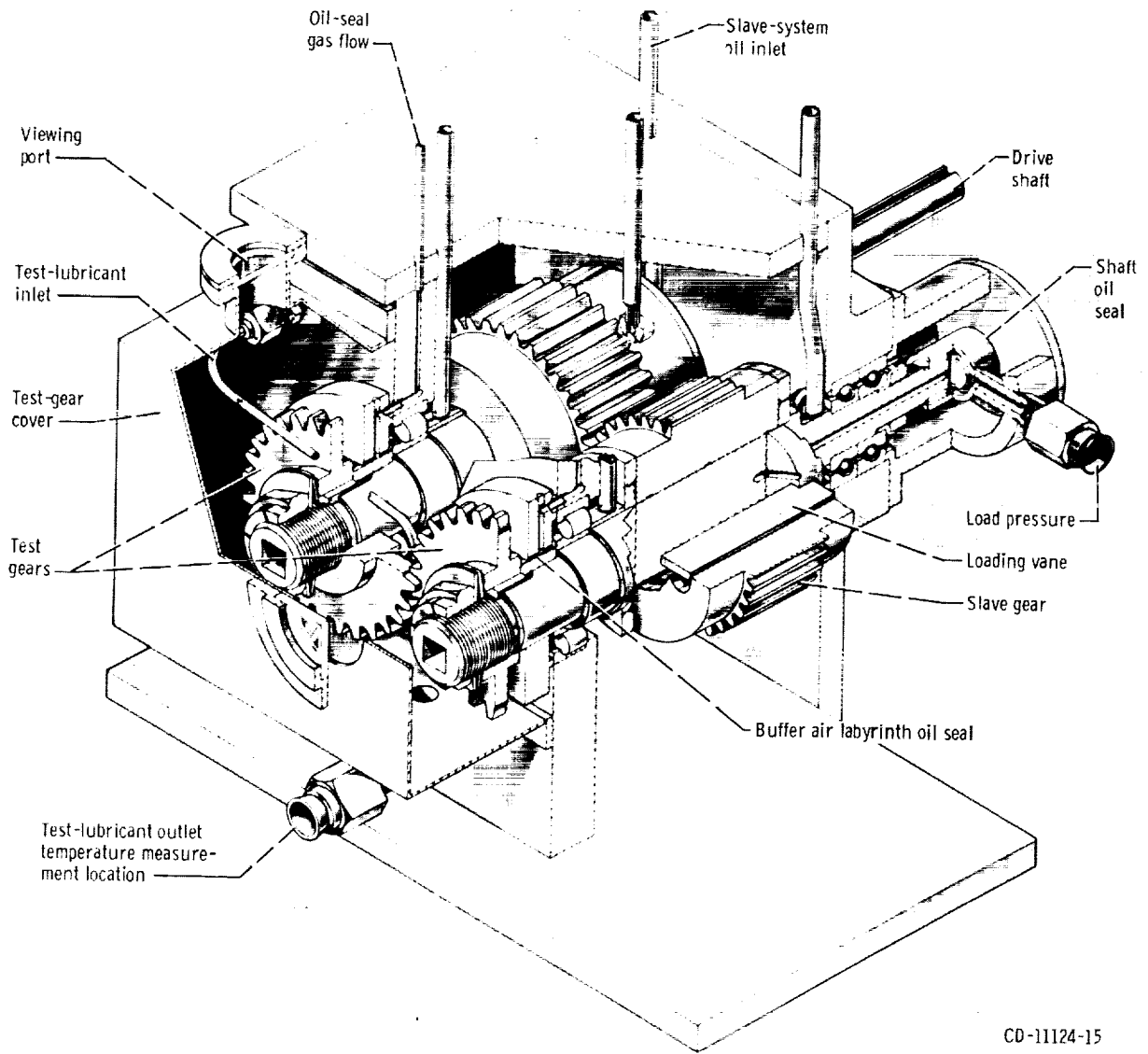
ARC REMELTED (VAR) AISI 9310

Step	Process	Temperature		Time, hr
		K	°F	
1	Carburize	1172	1650	8
2	Air cool to room temperature	----	----	---
3	Copper plate all over	----	----	---
4	Reheat	922	1200	2.5
5	Air cool to room temperature	----	----	---
6	Austenitize	1117	1550	2.5
7	Oil quench	----	----	---
8	Subzero cool	189	-120	3.5
9	Double temperature	450	350	2 each
10	Finish grind	----	----	---
11	Stress relieve	450	350	2

TABLE V. - SPUR GEAR DATA

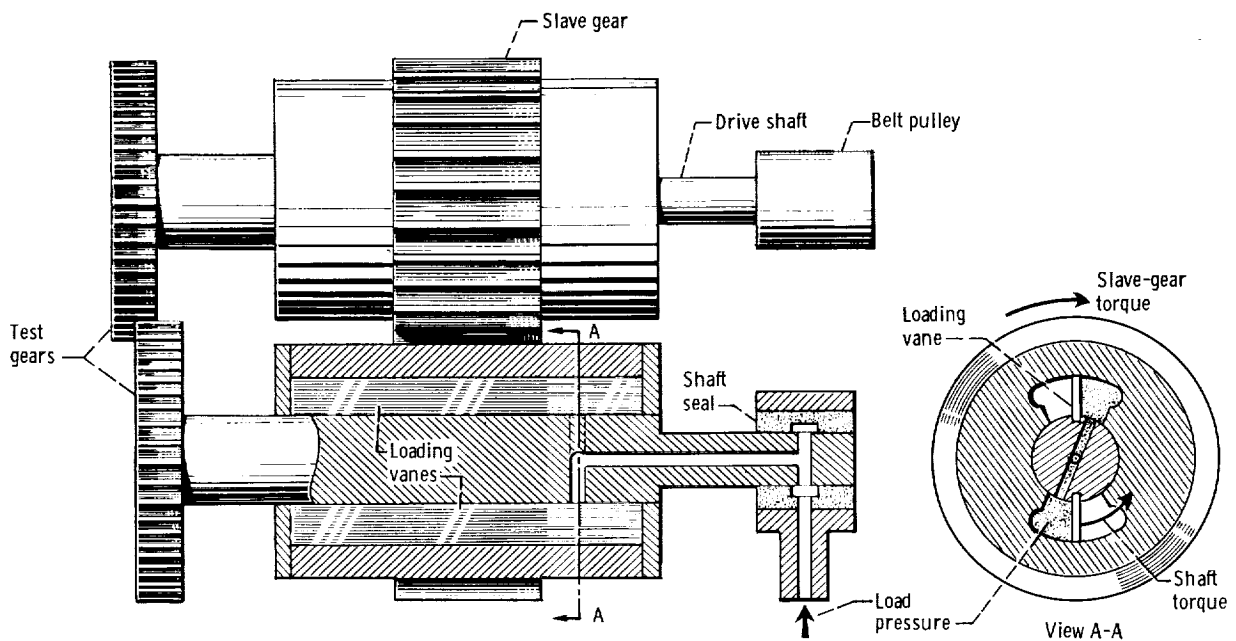
[Gear tolerance per ASMA class 12.]

Number of teeth	28
Diametral pitch	8
Circular pitch, cm (in.)	0.9975 (0.3927)
Whole depth, cm (in.)	0.762 (0.300)
Addendum, cm (in.)	0.318 (0.125)
Chordal tooth thickness reference, cm (in.)	0.485 (0.191)
Pressure angle, deg	20
Pitch diameter, cm (in.)	8.890 (3.500)
Outside diameter, cm (in.)	9.525 (3.750)
Root fillet, cm (in.)	0.102 to 0.152 (0.04 to 0.06)
Measurement over pins, cm (in.)	9.603 to 9.630 (3.7807 to 3.7915)
Pin diameter, cm (in.)	0.549 (0.216)
Backlash reference, cm (in.)	0.0254 (0.010)
Tip relief, cm (in.)	0.001 to 0.0015 (0.0004 to 0.0006)



CD-11124-15

Figure 1. - NASA Lewis Research Center's gear fatigue test apparatus.

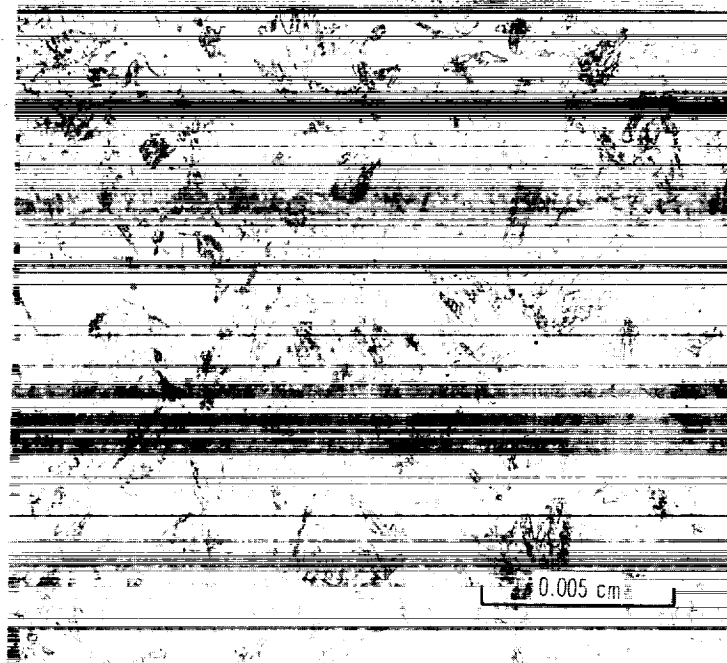


CD-11421-15

Figure 2 - Schematic diagram of gear fatigue apparatus.



(a) Carburized and hardened case of the VAR AISI 9310 gear showing high carbon fine grain martensitic structure.



(b) Core structure of VAR AISI 9310 gear showing low carbon refined austenitic grain size.

Figure 3. - Photomicrographs of case and core regions of test gears.

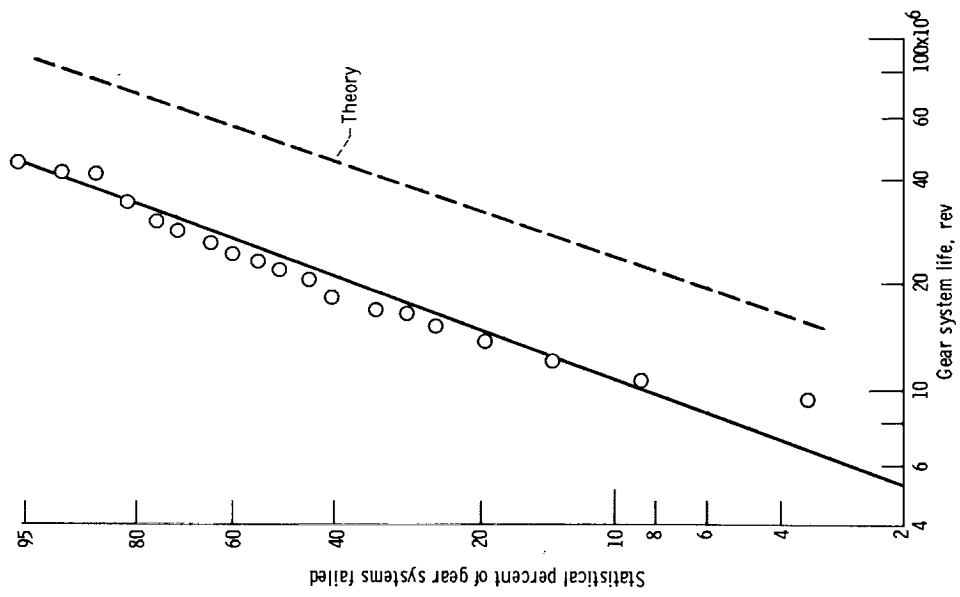


Figure 4. - Pitting fatigue lives of spur gear systems made of VAR AISI 9310. Maximum Hertz stress, 1.71×10^9 newtons (248 000 psi); speed, 10 000 rpm; temperature, 350 K (170° F); lubricant, superrefined naphthenic mineral oil; Weibull slope, 2.75.

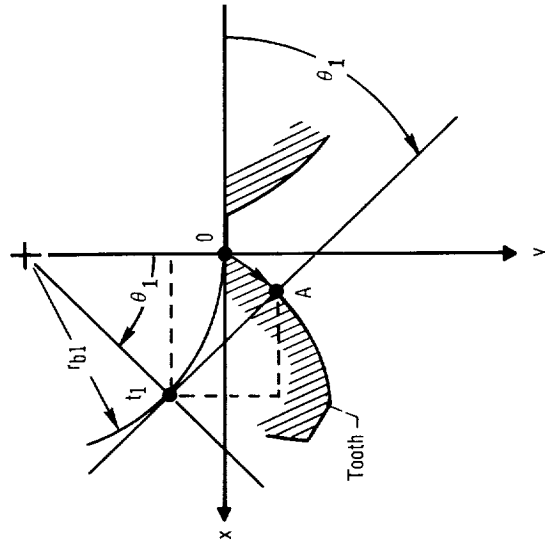


Figure 5. - Involute profile length.

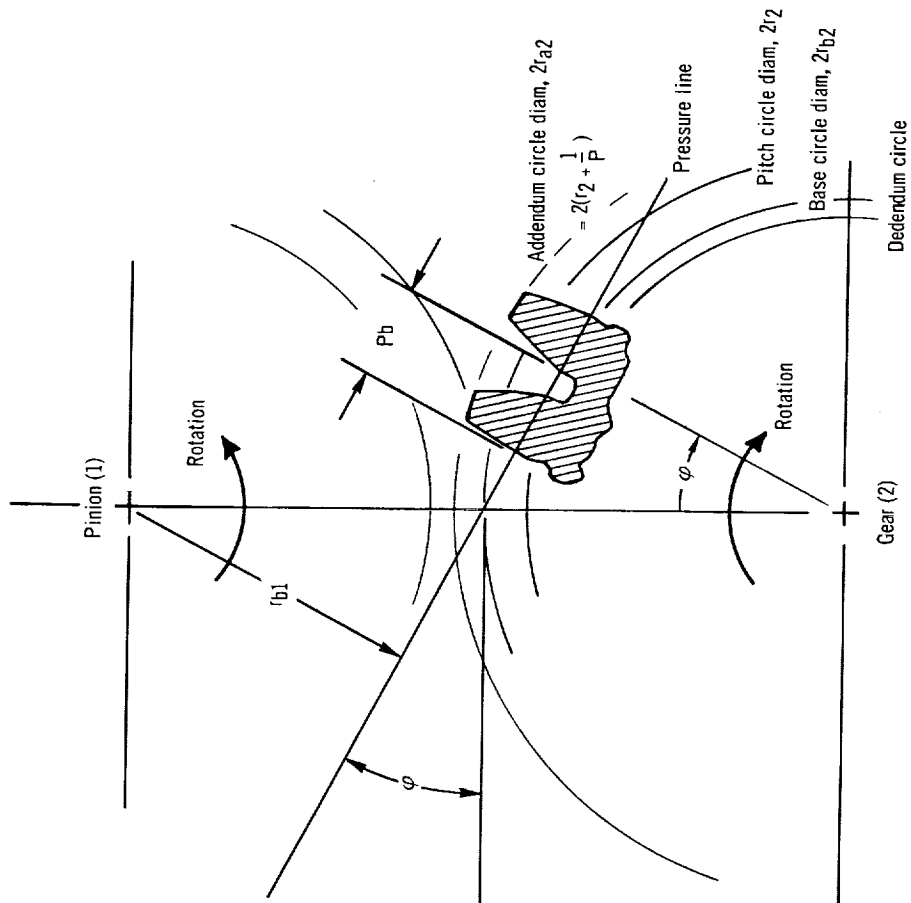


Figure 6. - Spur gears in mesh.

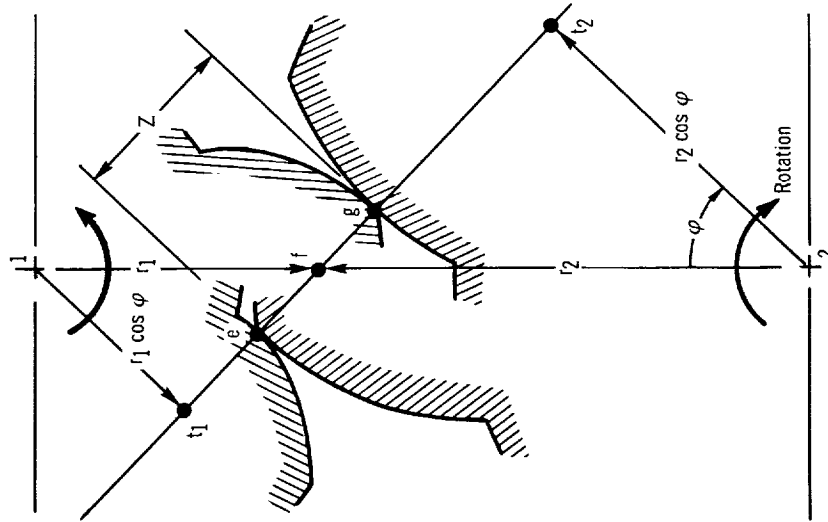


Figure 7. - Length of contact path.

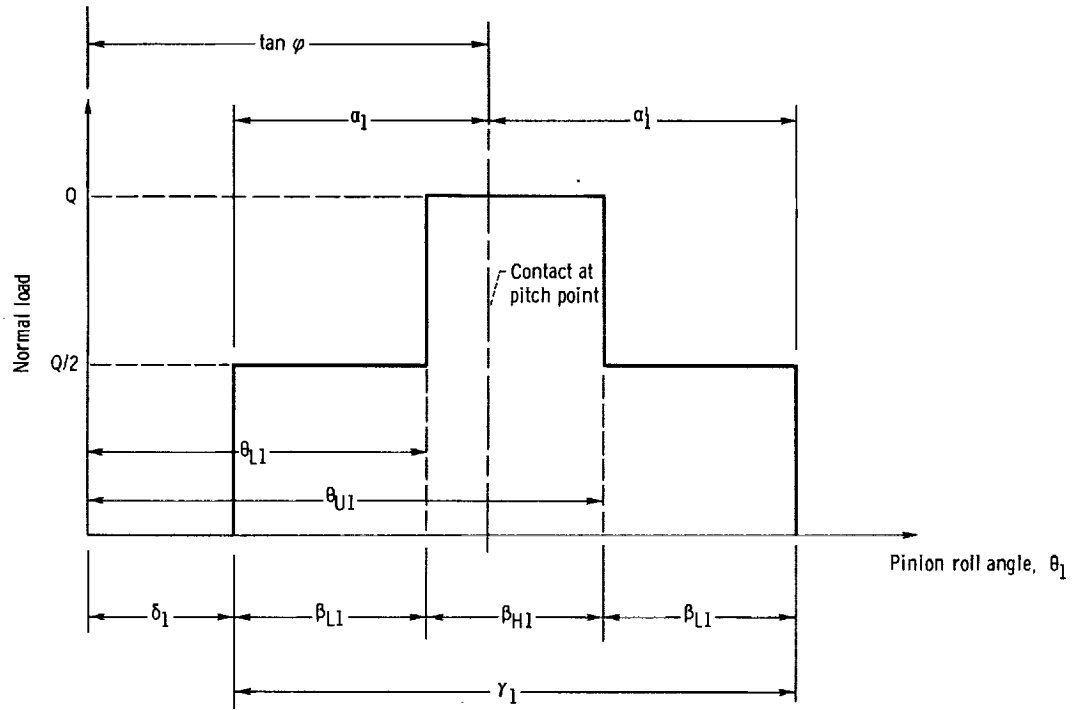


Figure 8. - Load sharing diagram. Load on tooth for low contact ratio gear depends on roll angle.

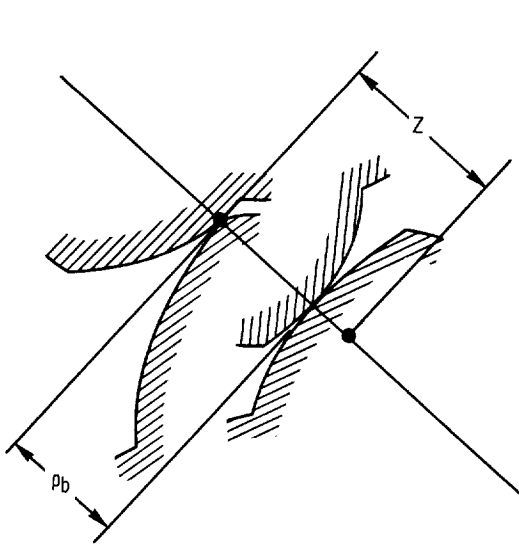


Figure 9. - Teeth coming into contact.

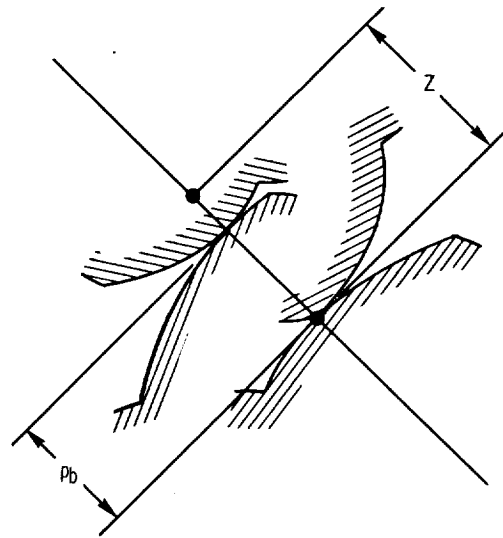


Figure 10. - Teeth going out of contact.

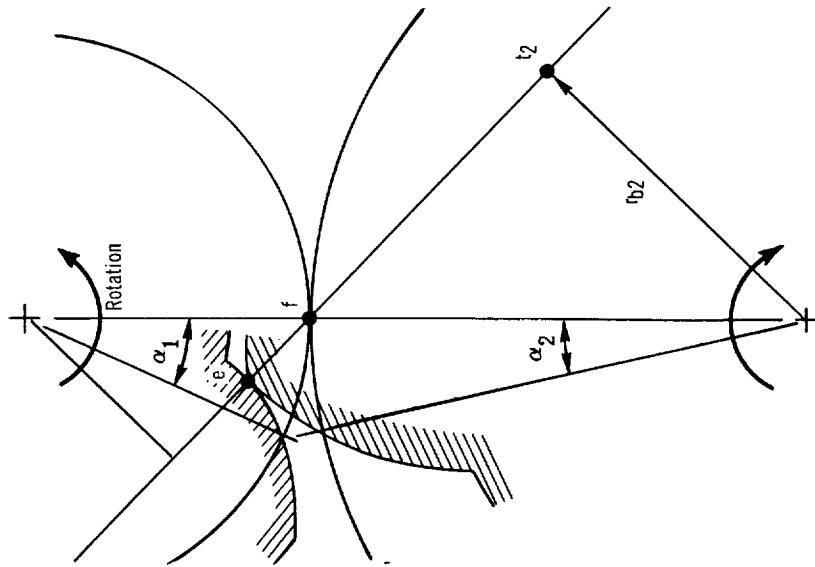


Figure 11. - Angle of approach.

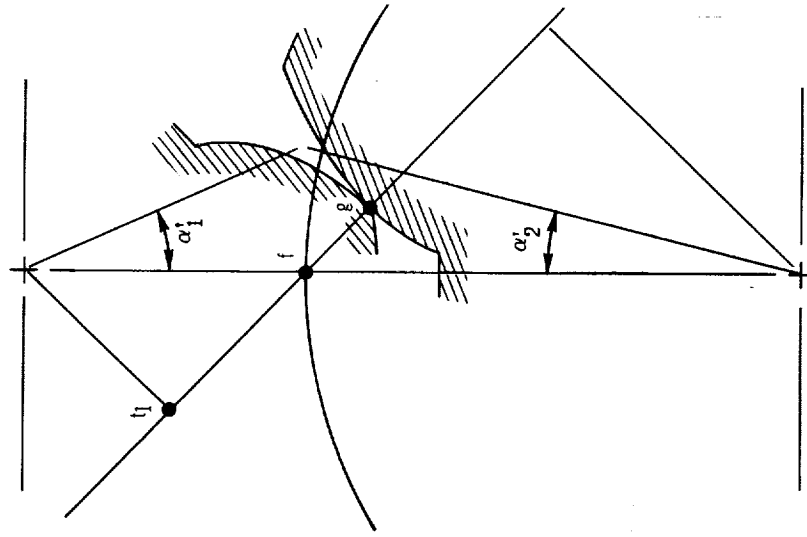


Figure 12. - Angle of recess.

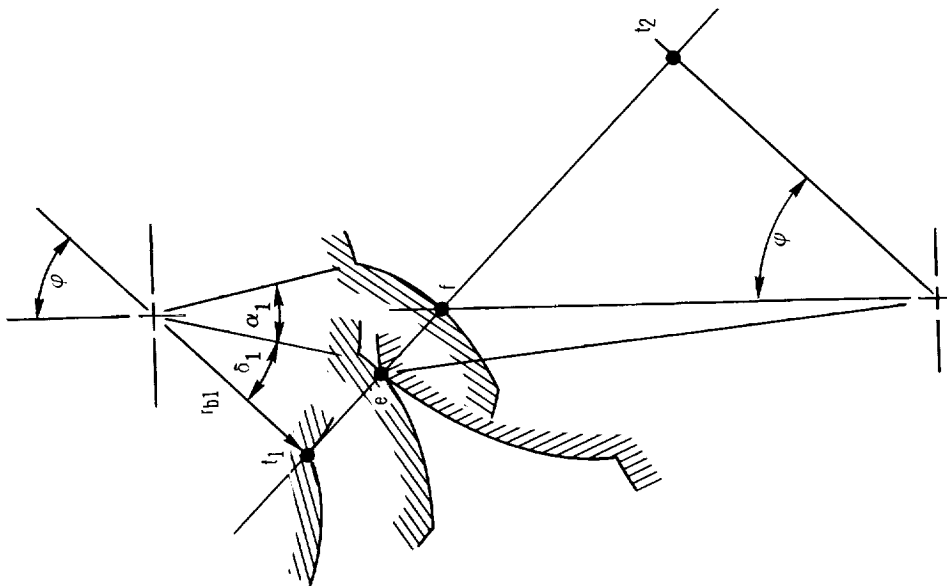


Figure 13. - Calculation of δ_1 .

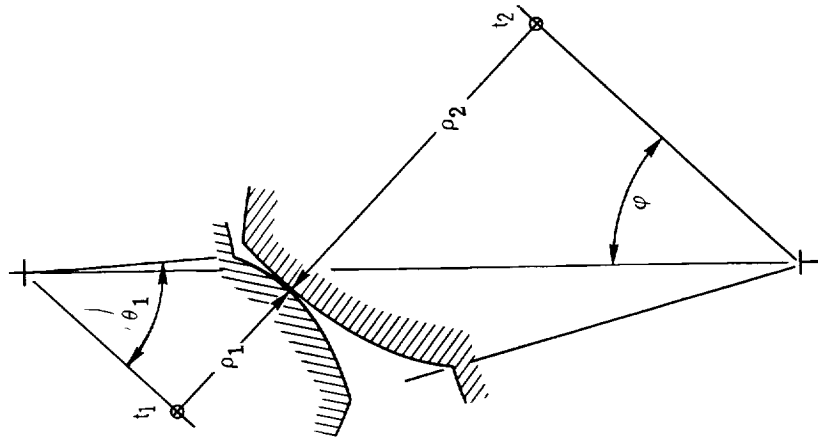


Figure 14. - Curvatures of involutes in contact.

1
2
3
4
5
6
7
8
9
10
11
12
13
14
15
16
17
18
19
20
21
22
23
24
25
26
27
28
29
30
31
32
33
34
35
36
37
38
39
40
41
42
43
44
45
46
47
48
49
50
51
52
53
54
55
56
57
58
59
60
61
62
63
64
65
66
67
68
69
70
71
72
73
74
75
76
77
78
79
80
81
82
83
84
85
86
87
88
89
90
91
92
93
94
95
96
97
98
99
100

1
2
3
4
5
6
7
8
9
10
11
12
13
14
15
16
17
18
19
20
21
22
23
24
25
26
27
28
29
30
31
32
33
34
35
36
37
38
39
40
41
42
43
44
45
46
47
48
49
50
51
52
53
54
55
56
57
58
59
60
61
62
63
64
65
66
67
68
69
70
71
72
73
74
75
76
77
78
79
80
81
82
83
84
85
86
87
88
89
90
91
92
93
94
95
96
97
98
99
100

